A Numerical Technique for SAW Diffraction Simulation

DAVID PENUNURI

Abstract—**An efficient numerical technique is presented for simulating the effect of diffraction on the performance of surface acoustic wave (SAW) devices. A computer code based on this technique accurately predicts the performance of several "practical" bandpass filters fabricated on ST-cut quartz. Since the algorithm is fast, an iterative design procedure which minimizes the frequency sidelobes in the presence of diffraction is now practical.**

I. Introduction

EVEN AS the specifications for SAW devices become more exacting, diffraction effects continue to plague device design, particularly low sidelobe narrow bandwidth filters. Diffraction begins to have deleterious effects as the specified sidelobe suppression level surpasses 40 dB in a single filter device and is almost exclusively the source of error at the 50-dB sidelobe level on ST-cut quartz.

Several approaches have been used to eliminate, or at least reduce, diffraction effects. The discovery of minimum diffraction cuts on bismuth germanium oxide (BGO) and lithium tantalate ($LiTaO_3$) [1], [2] has resulted in perhaps the best "simple" bandpass filters, in the sense that the experimental and theoretical (based on transversal filter calculations) frequency responses are very close [3]. By "simple" is meant a device consisting of one apodized transducer and one unapodized transducer. Unfortunately, these substrate materials are neither temperature compensated nor inexpensive.

Another approach has been to avoid apodization in filter design, instead, by making use of finger withdrawal to achieve spectral weighting [4]. This technique avoids very narrow finger overlaps which tend to be dominated by end effects [5], and are subject to severe diffraction errors. The disadvantage is that the transducers tend to have many more finger pairs than those of conventionally apodized transducers of the same fractional bandwidth. Finally, these devices are ultimately subject to substantial diffraction effects because, since the transducers are long and substrate size is constrained, it is difficult to design such transducers that are entirely within the near field or far field.

The last approach has been to retain a "simple" filter configuration, but correct the time sampling to compensate for diffraction effects. Because of current photolithographic constraints, it is generally not possible to accurately correct for phase errors, i.e., adjust the relative finger pair positions with sufficient resolution. Consequently, only amplitude correction has been investigated in depth, and only to demonstrate a 40-dB sidelobe level [6]. The disadvantages of this technique are that: 1) the compensation can be done exactly at one frequency only, e.g., the center frequency of the filter, because the diffraction pattern is in general a strong function of frequency, thus frequency sidelobes are not exactly corrected; 2) the diffraction phase errors (deviation from plane wave phase) remain, and can cause significant departure from the ideal response; and 3) after compensation for amplitude, it is extremely expensive to compute the response of a practical filter (fractional bandwidth less than a few percent) under the influence of diffraction in order to determine the effect of phase error. Thus an efficient numerical technique is required for the computation of a filter response, taking into account the complete diffraction problem. Then it becomes possible to analyze a filter design which has been derived by using the compensation techniques available, for example, or optimize an initial design by adjusting the apodization function and the center-to-center spacing of the transducers. With such a numerical algorithm, it becomes feasible to systematically adjust each finger overlap in order to maximize sidelobe suppression for a given transducer aperture and center-to-center spacing.

In this paper, such a numerical technique is presented which, under the conditions that the interdigital transducer can be modeled as an ideal transversal filter (conditions which are readily approached using ST-cut quartz and double electrode transducers) and that the SAW wave vector surface is parabolic (an assumption that is accurate for most substrates), permits the fast computation of the frequency response. No attempt is made to model any of the electromechanical or external circuit effects which are present in actual devices. In Section II the technique is derived, and in Section III an analysis of several experimental devices is presented.

II. Diffraction Formalism

Following the formalism established by Szabo and Slobodnik [7], we consider the response of a single antenna in the diffraction field due to a single line source on a half space. The aperture of the source is normalized to unity and only those antennas of aperture less than or

Manuscript received March 21, 1977; revised September 15, 1977.
The author is with Rockwell International, Electronics Research Center, Anaheim, CA 92803.

0018-9480/78/0400-0288$00.75

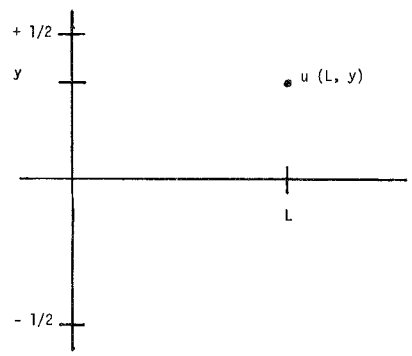

Fig. 1. Coordinate system for diffraction problem.

equal to unity are considered, as seen in Fig. 1. Note that the vertical axis is in units of aperture and the horizontal axis is in units of wavelength. The source is assumed to consist of a constant amplitude distribution. Then the amplitude $u(L,y)$ at any point $(L,y), L \geq 0, |y| \leq 1/2$, relative to a plane wave, is given by

$$\text{Re } u(L,y) = \text{Ci}(\theta) - \text{Ci}(\psi) \tag{1}$$

$$\text{Im } u(L,y) = \text{Si}(\psi) - \text{Si}(\theta) \tag{2}$$

where

$$\theta = \pi \frac{(y+1/2)^2}{|1+\gamma|} \frac{A^2}{L} \tag{3}$$

$$\psi = \pi \frac{(y-1/2)^2}{|1+\gamma|} \frac{A^2}{L} \tag{4}$$

γ is the slope of the power flow angle, A is the actual maximum aperture in wavelengths, and L is the source-to-antenna separation in wavelengths. Re and Im signify the real and imaginary parts, respectively, of a complex number. The functions $\text{Ci}(x)$ and $\text{Si}(x)$ are the Fresnel integrals usually defined as

$$\text{Ci}(x) = \frac{1}{\sqrt{2\pi}} \int_0^x \frac{\cos(t)}{\sqrt{t}}\, dt \tag{5}$$

$$\text{Si}(x) = \frac{1}{\sqrt{2\pi}} \int_0^x \frac{\sin(t)}{\sqrt{t}}\, dt. \tag{6}$$

Then the total response of an antenna of width $2Y$ centered on the beam axis at L is $U(L,Y)$ where

$$U(L,Y) = \int_{-Y}^{Y} u(L,y)\, dy \tag{7}$$

which can be written as

$$\text{Re } U(L,Y) = \alpha \int_{\Psi}^{\Theta} \frac{\text{Ci}(t)}{\sqrt{t}}\, dt \tag{8}$$

$$\text{Im } U(L,Y) = -\alpha \int_{\Psi}^{\Theta} \frac{\text{Si}(t)}{\sqrt{t}}\, dt \tag{9}$$

where

$$\Theta = \left(\frac{Y+1/2}{\alpha}\right)^2 \tag{10}$$

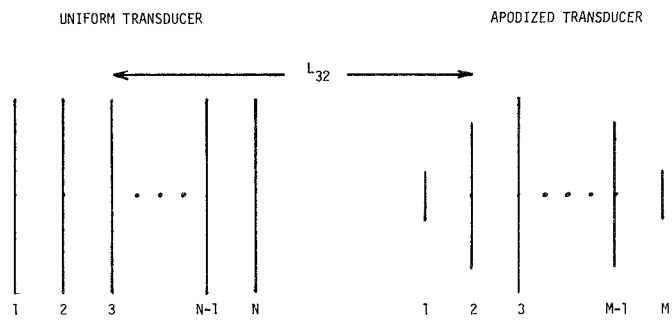

Fig. 2. "Simple" filter configuration.

$$\Psi = \left(\frac{Y-1/2}{\alpha}\right)^2 \tag{11}$$

$$\alpha = \left(\frac{|1+\gamma 1}{\pi} \frac{L}{A^2}\right)^{1/2}. \tag{12}$$

In order to facilitate the numerical computation, two new functions are defined as

$$\text{Cii}(x) = \int_0^x \frac{\text{Ci}(t)}{\sqrt{t}}\, dt \tag{13}$$

$$\text{Sii}(x) = \int_0^x \frac{\text{Si}(t)}{\sqrt{t}}\, dt \tag{14}$$

which, for brevity, we call the second Fresnel integrals. Then the total response at the antenna is rewritten

$$\frac{1}{\alpha} \text{Re } U(L,Y) = \text{Cii}(\theta) - \text{Cii}(\Psi) \tag{15}$$

$$\frac{1}{\alpha} \text{Im } U(L,Y) = \text{Sii}(\Psi) - \text{Sii}(\theta). \tag{16}$$

These expressions can be further simplified so that the responses of the many finger pair filters can be written compactly. We define

$$\text{Eii}(x) = \text{Cii}(x) + j\,\text{Sii}(x) \tag{17}$$

and using the fact that

$$\text{Cii}(-x) = -\text{Cii}(x) \tag{18}$$

and

$$\text{Sii}(-x) = \text{Sii}(x) \tag{19}$$

we write the total response as

$$\frac{1}{\alpha} U(L,Y) = \text{Eii}(-\Psi) - \text{Eii}(-\Theta). \tag{20}$$

We assume that each finger pair of a SAW transducer is an independent line source. Then the response of a "simple" filter consisting of N uniform aperture sources and M variable aperture antennas as in Fig. 2 can be written as

$$U = \sum_{n=1}^{N} {}^{\sigma}n \sum_{m=1}^{M} {}^{\alpha}nm\,{}^{\hat{\sigma}}m\left(\text{Eii}(-{}^{\Psi}nm) - \text{Eii}(-{}^{\Theta}nm)\right) e^{-j2\pi p L nm} \tag{21}$$

where

$$\Theta nm = \left(\frac{Ym+1/2}{{}^{\alpha}nm}\right)^2 \tag{22}$$

TABLE I
COMPARISON OF NUMBER OF OPERATIONS REQUIRED TO COMPUTE FRESNEL INTEGRAL AND SECOND FRESNEL INTEGRAL

Function	sin(x)	cos(x)	X	+	$\sqrt{\ }$
Fresnel Int.	1	1	22	26	1
Second Fresnel Int.	1	1	43	45	1

$$\Psi_{nm}=\left(\frac{Ym-1/2}{\alpha_{nm}}\right)^2 \tag{23}$$

$$\alpha_{nm}=\left(\frac{1+\gamma}{\pi}\cdot\frac{L_{nm}}{\rho A_0^2}\right)^{1/2}. \tag{24}$$

N and M are the number of finger pairs in the uniform and apodized aperture transducers, respectively, and σ_n and σ_m are the signs (+ or −) of the nth and mth finger pairs of the uniform and apodized transducers, respectively.

$$L_{nm}=L_0+\frac{N-M}{2}-n+m. \tag{25}$$

L_0 is the center-to-center spacing between transducers in wavelengths at the fundamental frequency, A_0 is the aperture in wavelengths at the fundamental frequency, and $\rho=f/f_0$, where f is the frequency and f_0 is the fundamental frequency.

It is shown in the Appendix that Cii(x) and Sii(x), or equivalently, Eii(x), can be computed simultaneously using polynomial approximations. By comparison, a "brute force" computation [8] would require that each finger pair of the apodized transducer be divided into a large number of small sections. The field at the center of each section would be computed and all such contributions would be summed to yield the response of a finger pair. The fact that the fields must be evaluated at many points, e.g., P, along the aperture of a finger pair, implies that the Fresnel integrals must be computed P times. Using the algorithm proposed in this paper, the second Fresnel integrals must be computed only once for the response of the finger pair in question. Thus the relative advantage of the new method is obvious if the number of similar operations required to compute the Fresnel integrals and the second Fresnel integrals are compared as in Table I. The algorithms are seen to be quite similar in terms of computational effort. Based on reasonable estimates of the relative time required to perform the various operations and compute the sine, cosine, and square-root functions, a single evaluation of the second Fresnel integral algorithm requires at most 50-percent more computation than a single evaluation of the Fresnel integral algorithm. Thus it is concluded that the new method is more efficient by essentially a factor of $P/1.5$ because the numerical quadrature for each finger pair is eliminated. This savings is significant since, for a reasonable approximation of about three significant digits in the quadrature along the aperture, we must have $20 \leqslant P \leqslant 50$. Thus (21) is a fast computational algorithm for computing the filter response in the presence of diffraction effects.

TABLE II
BANDPASS FILTER SPECIFICATIONS

Filter	Center Frequency (MHz)	Max. Aperture (λo)	Center-To-Center Spacing (λo)	N	M
#1	65.8	41	330.0	35	160
#2	28.2	30	330.0	64	100
#3	65.8	90	291.0	26	120
#4	121.3	50	372.7	65	192

III. COMPARISON OF THEORY AND EXPERIMENT

Four bandpass filters were fabricated on ST-cut quartz with the specifications seen in Table II. The table shows the center frequency at the fundamental, the maximum aperture in fundamental wavelengths, the center-to-center spacing of the transducers, and the number of finger pairs in each transducer. All filters consisted of interdigital transducers with double electrodes of aluminum metallization 1000 Å thick. The apodized transducers contained dummy electrodes starting two wavelengths from the end of each active electrode. All frequency response measurements were made in a 50-Ω system with no matching circuits of any kind. The transducer apodization for each filter was based on a simple summation of plane waves or discrete Fourier transform analysis with no modification. For the purposes of this paper, filters 1 and 3 were studied at their fundamental frequency only. Filters 2 and 4 were studied both at the fundamental and at the third harmonic. The table shows that these devices are typical of IF filters which might be encountered in practical applications, with 100–200 finger pairs in the apodized transducer and fractional bandwidths in the range 0.5–5 percent.

Figs. 3–8 show the frequency response for each filter which was expected on the basis of a plane wave analysis (solid line), the experimental response (dashed line), and the calculated response, including diffraction using the algorithm described above with $\gamma=0.378$ (open squares). The figures show only the high frequency side of the bandpass since the low frequency side is similar. Many more points were computed than are indicated by the number of open squares on each figure. The experimental response is considerably degraded from the ideal response for all filters. The sidelobes are higher by as much as 30 dB and are "smeared" together by diffraction. Furthermore, in all cases except for filter 2 at the fundamental, the experimental response was accurately predicted (within 2 dB) solely by including the effect of diffraction. The uniform transducer for filter 2 contained sections of phase-reversed finger pairs. As has been discussed by Smith [9] such devices tend to exhibit frequency responses

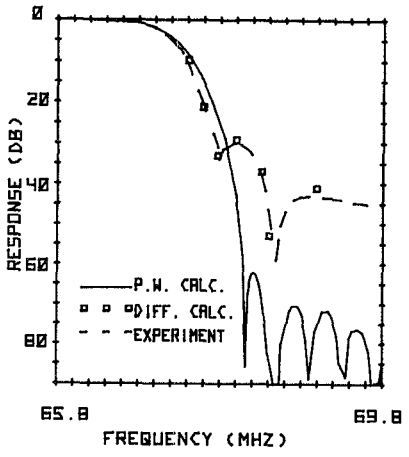

Fig. 3. Frequency response of filter 1, based on summation of plane waves (solid line), including diffraction using new technique (open squares) and experiment (dashed line).

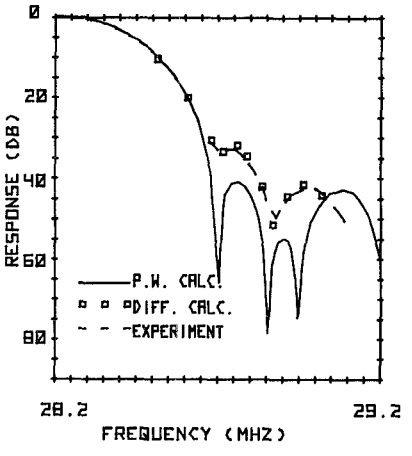

Fig. 4. Frequency response of filter 2 at the fundamental.

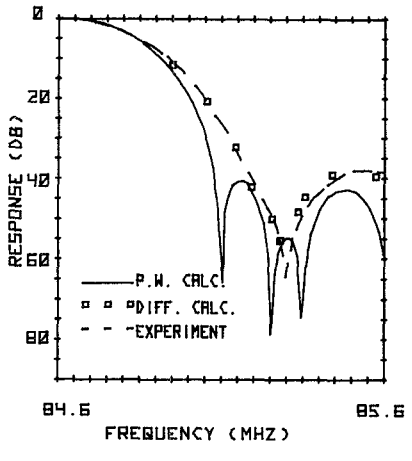

Fig. 5. Frequency response of filter 2 at the third harmonic.

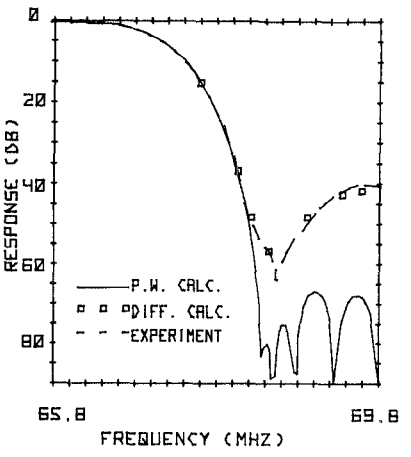

Fig. 6. Frequency response of filter 3.

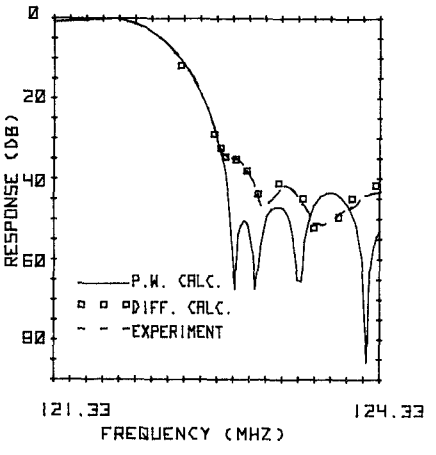

Fig. 7. Frequency response of filter 4 at the fundamental.

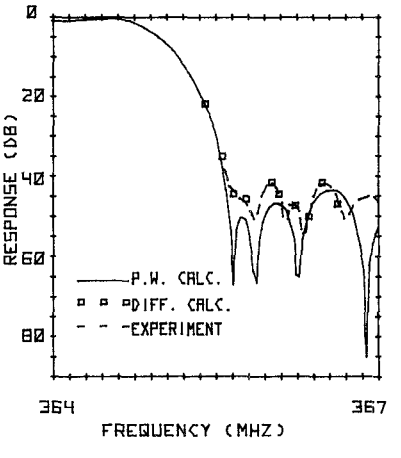

Fig. 8. Frequency response of filter 4 at the third harmonic.

which are skewed relative to the center frequency. This effect was observed for filter 2 and resulted in as much as a 7-dB deviation between the experimental response and that predicted using the diffraction analysis, although there was qualitative agreement. When the experimental response was averaged about center frequency in order to eliminate the bandpass skewing, the disagreement was reduced to less than 2 dB.

IV. Conclusion

A numerical technique was presented which permits the fast computation of the frequency response of SAW devices under the assumption that an interdigital transducer can be modeled as an ideal transversal filter and that the diffraction is parabolic. The technique reduces the computational effort by a large factor (20–50) relative to a typical "brute force" method.

The numerical code induced by the algorithm was used to accurately predict the frequency response of several bandpass filters. The filters were "practical" in the sense that the transducers consisted of a large number of finger pairs (100–200). The experimental and theoretical frequency responses were typically within 2 dB. These results illustrate the fact that the major source of error on ST-quartz is diffraction.

Finally, we note that since the new method is very efficient, a true optimizing design procedure is now practical. It is now possible to analyze an initial design very quickly, systematically modify the finger overlaps, and reanalyze. Thus, as an example, it should be possible to iteratively search for a maximum in the sidelobe suppression level.

V. Appendix

Computation of Eii(x)

The numerical evaluation of Eii(x) as defined in (13) and (14) is based on a polynomial approximation for the Fresnel integrals, Ci(x) and Si(x) [10]. By substituting these approximations into the integrand of (13) and (14), it becomes possible to evaluate the integrals exactly. This procedure leads to a polynomial approximation for Cii(x) and Sii(x). The numerical approximation of the Fresnel integrals in [10] is presented for two ranges of the argument, $|x| \leqslant 4$ and $|x| > 4$. Therefore, the evaluation of Cii(x) and Sii(x) is considered separately over similar ranges except that only $x \geqslant 0$ need be considered.

In the range $0 \leqslant x \leqslant 4$, the Fresnel integrals are approximated by

$$\mathrm{Ci}(x) = \sqrt{x} \sum_{m=0}^{6} c_m x^{2m} \tag{A1}$$

and

$$\mathrm{Si}(x) = \sqrt{x} \sum_{m=0}^{5} d_m x^{2m+1} \tag{A2}$$

where the coefficients c_m and d_m are tabulated in [9]. Therefore

$$\mathrm{Cii}(x) = \sum_{m=0}^{6} c'_m x^{2m+1} \tag{A3}$$

and

$$\mathrm{Sii}(x) = \sum_{m=0}^{5} d'_m x^{2m+2} \tag{A4}$$

where $c'_m = c_m/(2m+1)$ and $d'_m = d_m/(2m+2)$. The new coefficients c'_m and d'_m appear in Table III.

In the range $x > 4$, we write

TABLE III
Coefficients of Cii(x) and Sii(x) for the Range $0 \leqslant x \leqslant 4$; Parenthesis Contain Base 10 Exponent

m	c'_m	d'_m
0	7.9788455 (-1)	1.3298075 (-1)
1	-2.6596135 (-2)	-4.7492775 (-3)
2	7.3877172 (-4)	1.0072562 (-4)
3	-1.2174946 (-5)	-1.3157316 (-6)
4	1.2894760 (-7)	1.1225331 (-8)
5	-9.2188446 (-10)	5.5647873 (-11)
6	3.9229499 (-12)	0

$$\mathrm{Cii}(x) = \mathrm{Cii}(4) + \int_4^x \frac{\mathrm{Ci}(t)}{\sqrt{t}}\, dt \tag{A5}$$

and

$$\mathrm{Sii}(x) = \mathrm{Sii}(4) + \int_4^x \frac{\mathrm{Si}(t)}{\sqrt{t}}\, dt. \tag{A6}$$

The first term of the RHS for both functions is obtained by evaluating the approximations obtained above for $0 \leqslant x \leqslant 4$. In order to evaluate the remaining integral we make use of the approximations

$$\mathrm{Ci}(x) = \frac{1}{2} + \frac{2}{\sqrt{x}} \{\cos(x) P(x) + \sin(x) Q(x)\} \tag{A7}$$

$$\mathrm{Si}(x) = \frac{1}{2} + \frac{2}{\sqrt{x}} \{\sin(x) P(x) - \cos(x) Q(x)\} \tag{A8}$$

with

$$P(x) = \sum_{m=0}^{8} \frac{4^m b_m}{x^m} \tag{A9}$$

and

$$Q(x) = \sum_{m=0}^{7} \frac{4^m a_m}{x^m}. \tag{A10}$$

The coefficients a_m and b_m are tabulated in [10]. Substituting (A7)–(A10) into (A5) and (A6) and performing the integration yields

$$\begin{aligned}\mathrm{Cii}(x) = \mathrm{Cii}(4) &+ \sqrt{x} - 2 \\ &+ 2 \sum_{m=0}^{8} 4^m b_m \{C_{m+1}(x) - C_{m+1}(4)\} \\ &+ 2 \sum_{m=0}^{7} 4^m a_m \{S_{m+1}(x) - S_{m+1}(4)\}\end{aligned} \tag{A11}$$

with a similar result for Sii(x), where we have defined

$$C_m(x) = \int_\infty^x \frac{\cos(t)}{t^m}\, dt \tag{A12}$$

and

$$S_m(x) = \int_\infty^x \frac{\sin(t)}{t^m}\, dt. \tag{A13}$$

It can be shown via integration by parts that the functions $C_m(x)$ and $S_m(x)$ satisfy the recursive relations

$$C_{m+1}(x) = -\frac{\cos(x)}{m x^m} - \frac{S_{m(x)}}{m} \tag{A14}$$

and

$$S_{m+1}(x) = -\frac{\sin(x)}{mx^m} + \frac{C_m(x)}{m} \tag{A15}$$

for $m \geq 1$. The starting functions are

$$C_1(x) = \int_{\infty}^{x} \frac{\cos(t)}{t}\, dt \triangleq \mathrm{Ci}(x) \tag{A16}$$

and

$$S_1(x) = \int_{\infty}^{x} \frac{\sin(t)}{t}\, dt \triangleq \mathrm{Si}(x) \tag{A17}$$

which are the well-known cosine and sine integrals. Algebraic manipulation of the expression for Cii(x) in (A11) and the similar result for Sii(x) yields the simplified expressions

$$\mathrm{Cii}(x) = C_0 + \sqrt{x} + \sum_{m=0}^{8} \{b'_m C_{m+1}(x) + a'_m S_{m+1}(x)\} \tag{A18}$$

and

$$\mathrm{Sii}(x) = S_0 + \sqrt{x} + \sum_{m=0}^{8} \{b'_m S_{m+1}(x) - a'_m C_{m+1}(x)\} \tag{A19}$$

where

$$a'_m = 2(4^m a_m), \qquad m = 0, 1, \cdots, 7$$
$$a'_8 = 0$$

and

$$b'_m = 2(4^m b_m), \qquad m = 0, 1, \cdots, 8.$$

C_0 and S_0 are constants.

In order to speed up the algorithm defined by (A14)–(A19), we eliminate the recursive computation in (A14) and (A15) by noting that we can write

$$C_m(x) = C_m S_1(x) + D_m C_1(x) + \sin(x) \sum_{k=1}^{8} \frac{c_{mk}}{x^k} + \cos(x) \sum_{k=1}^{8} \frac{d_{mk}}{x^k} \tag{A20}$$

$$S_m(x) = A_m S_1(x) + B_m C_1(x) + \sin(x) \sum_{k=1}^{8} \frac{a_{mk}}{x^k} + \cos(x) \sum_{k=1}^{8} \frac{b_{mk}}{x^k} \tag{A21}$$

where A_m, B_m, C_m, D_m, a_{mk}, b_{mk}, c_{mk}, and d_{mk} are constants that are readily determined from (A14) and (A15). Substitution of (A20) and (A21) into (A18) and (A19) and collecting the sums yields the final result

$$\mathrm{Cii}(x) = C_0 + \sqrt{x} - P_0 S_1(x) + Q_0 C_1(x) - \sin(x) \sum_{k=1}^{8} \frac{U_k}{x^k} + \cos(x) \sum_{k=1}^{8} \frac{T_k}{x^k} \tag{A22}$$

$$\mathrm{Sii}(x) = S_0 + \sqrt{x} + Q_0 S_1(x) + P_0 C_1(x) + \sin(x) \sum_{k=1}^{8} \frac{T_k}{x^k} + \cos(x) \sum_{k=1}^{8} \frac{U_k}{x^k} \tag{A23}$$

TABLE IV
COEFFICIENTS OF Cii(x) AND Sii(x) FOR THE RANGE $x > 4$; PARENTHESIS CONTAIN BASE 10 EXPONENT

k	U_k	T_k
1	-1.8544377(-1)	6.8450242 (-1)
2	-4.850367 (-1)	-2.0538677 (-1)
3	4.1128759 (-1)	-6.7199626 (-1)
4	1.2515535	1.2854102
5	-4.9831594	1.202952
6	7.8968972	-1.0023376 (1)
7	-5.1577087	1.951704 (1)
8	0	-1.4365914 (1)

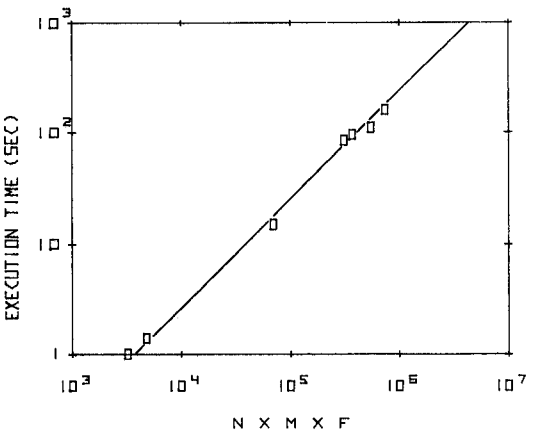

Fig. 9. Execution time for Fortran IV computer program inplementation of proposed diffraction algorithm using an IBM System370/model 168 machine. N = number of finger pairs in uniform transducer, M = number of finger pairs in apodized transducer, and F = number of frequency points to be calculated. Open squares represent some actual computations.

where

$$C_0 = 2.93 \times 10^{-9}$$
$$S_0 = -0.79601733$$
$$P_0 = -1.083445$$
$$Q_0 = -0.2053964.$$

The coefficients U_k and T_k are presented in Table IV. The sine and cosine integrals $S_1(x)$ and $C_1(x)$ can be computed using polynomial approximations also available in [9].

This section is concluded with a few remarks concerning the computer implementation of (A22) and (A23), since the exact details of encoding will dramatically affect the speed of execution. It should be noted that: 1) the evaluation of $S_1(x)$ and $C_1(x)$ (sine and cosine integrals) should *not* be performed in a separate subprogram in order to reduce the number of $\sin(x)$ and $\cos(x)$ valuations from two each to one each, 2) the two polynomials in (A22) and (A23) should be evaluated using Horner's nested form for maximum speed and accuracy [11], and 3) an optimizing compiler should be used for maximum speed. The numerical algorithm proposed in this paper was implemented in a Fortran IV computer program. The execution time is illustrated in Fig. 9 as a function of the product NMF, where N is the number of finger pairs in the uniform transducer, M is the number of finger pairs in the apodized transducer, and F is the number of

frequency points to be computed. The calculations were performed on an IBM System/370 Model 168 machine.

ACKNOWLEDGMENT

The author wishes to thank L. R. Adkins for helpful discussions and L. Gray for fabricating the experimental devices.

REFERENCES

[1] A. J. Slobodnik, Jr. and T. L. Szabo, "Minimal diffraction cuts for acoustic surface wave propagation of $Bi_{12}GeO_{20}$," *J. Appl. Phys.*, vol. 44, no. 7, pp. 2937–2941, July 1973.
[2] A. J. Slobodnik, Jr., T. E. Fenstermacher, and W. J. Kearns, "A minimal diffraction lithium tantalate substrate for contiguous SAW butterworth filters," in *Proc. 1975 Ultrason. Symp.* pp. 405–407, IEEE Cat. #75 CHO 994-4SU.
[3] A. J. Slobodnik, J., K. R. Laker, and T. E. Fenstermacher, "A SAW filter with improved frequency and time domain characteristics for the frequency measurement of narrow-RF pulses," in *Proc. 1975 Ultrason. Symp.*, pp. 327–330, IEEE Cat. #75 CHO 994-4SU.
[4] R. S. Wagers, "SAW diffraction analysis by paired echo superposition," *IEEE Trans. Sonics Ultrason.*, vol. SU-23, pp. 249–254, July 1976.
[5] ——"Transverse electrostatic end effects in interdigital transducers," in *Proc. 1976 Ultrason. Symp.*, pp. 536–539, IEEE Cat. #76 CH1120-5SU.
[6] T. L. Szabo and A. J. Slobodnik, Jr., "Diffraction compensation in periodic apodized acoustic surface wave filters," *IEEE Trans. Sonics Ultrason.*, vol. SU-21, pp. 114–119, April 1974.
[7] ——"The effect of diffraction on the design of acoustic surface wave devices," *IEEE Trans. Sonics Ultrason.*, vol. SU-20, pp. 240–251, July 1973.
[8] R. F. Mitchell and R. Stevens, "Diffraction effects in small-aperture acoustic surface wave filters," *Wave Electron.*, vol. 1, pp. 201–218.
[9] W. R. Smith, Jr., "Circuit model analysis for interdigital transducers with arbitrary stripe-to-gap ratios, polarity sequences, and harmonic operation," in *Proc. 1974 Ultrason. Symp.*, IEEE Cat. #74 CHO 896-1SU.
[10] *System/360 Scientific Subroutine Package, Version III, Programmer's Manual*, International Business Machines Corp., Publication #H200205-3, 1968.
[11] E. K. Blum, *Numerical Analysis and Computation, Theory and Practice*. Reading, MA: Addison-Wesley, 1972.

Static Capacitance Calculations for a Surface Acoustic Wave Interdigital Transducer in Multilayered Media

ADRIAN VENEMA, JOZEF J. M. DEKKERS, AND R. F. HUMPHRYES

Abstract—**The static capacitance of an interdigital structure in multilayered media has been calculated. Numerical results are given for a surface acoustic wave interdigital transducer on an oxidized silicon substrate with a piezoelectric overlay. The capacitance is derived in terms of the layer thicknesses for zero and infinite substrate resistivity.**

SURFACE acoustic wave (SAW) generation and detection on a nonpiezoelectric substrate such as silicon necessitates a piezoelectric overlay [1]. Examples of commonly used overlay materials include cadmium sulphide and zinc oxide. If it is intended to incorporate SAW devices and electronic components monolithically on the same silicon slice, then for compatability with silicon planar technology the silicon must be oxidized. In fact this is an advantage because the silicon dioxide also acts as an insulator between the interdigital transducer (IDT) and the electrically conductive silicon, thus making such monolithic integration possible. On the other hand, the acoustic propagating medium is now further complicated by the additional layer.

There are four possible transducer configurations [2] for such a multilayered structure. This choice is halved when it is deemed necessary to optimize for maximum electromechanical coupling. The remaining two configurations require the IDT to be embedded between the thermally oxidized silicon substrate and the piezoelectric overlay. Furthermore, one of these requires a metal electrode (in the form of a platelet) to be depositied on the top of the piezoelectric overlay immediately above the IDT. The latter has advantages at low kh_2 values (k is SAW wavenumber, h_2 is piezoelectric layer thickness) where under certain conditions considerable enhancement is obtainable. At higher kh_2 values the performances of the two

Manuscript received May 2, 1977; revised August 16, 1977.

A. Venema is with the Department of Electrical Engineering, Delft University of Technology, Delft, The Netherlands.

J. J. M. Dekkers was with the Department of Electrical Engineering, Delft University of Technology, Delft, The Netherlands. He is now with the Institut für Halbleitertechniek, Rheinisch-Westfälische Technische Hochschule, Aachen, Germany.

R. F. Humphryes is with the Department of Electrical Engineering, Delft University of Technology, Delft, The Netherlands, on leave from Kelvin Hughes (Division of Smiths Industries Ltd.), Hainault, Essex, England.

0018-9480/78/0400-0294$00.75